

1 Rapidity dependence of identified charged hadrons  
2 in Au+Au collisions at  $\sqrt{s_{NN}} = 54.4$  GeV using the  
3 STAR detector

4 Arushi Dhamija (for the STAR Collaboration)<sup>1\*</sup>

5 <sup>1</sup>Department of Physics, Panjab University, Chandigarh (India)

6 \*arushidhamija507@gmail.com

7 July 22, 2023

8 **Abstract**

9 Exploring the QCD phase diagram and searching for the QCD critical point  
10 are some of the main goals of the Beam Energy Scan program at RHIC. In 2017,  
11 the STAR experiment collected a large dataset of Au+Au collisions at  $\sqrt{s_{NN}} =$   
12 54.4 GeV. The identified particle spectra and yields provide information about  
13 the bulk properties of the hot medium created in these collisions. Furthermore,  
14 the rapidity dependence study is essential for exploring the boost-invariant  
15 regions of the system.

16 We present the measurements of the production of  $\pi^\pm$ ,  $K^\pm$ ,  $p$ , and  $\bar{p}$  in  
17 various centralities and rapidity intervals. The results for the transverse mo-  
18 mentum spectra, particle yields  $dN/dy$ , average transverse momentum  $\langle p_T \rangle$ ,  
19 and particle ratios will be presented for different centrality classes and rapid-  
20 ity intervals. The kinetic freeze-out parameters will be obtained for different  
21 rapidity intervals and the results will be compared to similar measurements at  
22 other energies. The physics implications of the results will be discussed.

# 1 Introduction

The Beam Energy Scan (BES) Program at Relativistic Heavy Ion Collider (RHIC) aims to explore the Quantum Chromodynamics (QCD) critical point and phase boundary by varying collision energy [1]. The identified spectra and yields of charged hadrons provide insights into the bulk properties of the hot medium created in heavy-ion collisions [2]. In this study, we present charged hadron production ( $\pi^\pm$ ,  $K^\pm$ ,  $p$ ,  $\bar{p}$ ) at mid-rapidity ( $|y| < 0.1$ ) from Au+Au collisions at  $\sqrt{s_{NN}} = 54.4$  GeV, collected by the STAR experiment as part of the BES II program at RHIC.

# 2 Results and Discussion

Figure 1 illustrates the transverse momentum spectra for identified charged hadrons ( $\pi^+$ ,  $K^+$ , and  $p$ ) across nine centrality classes. The spectra are fitted using the Levy-Tsallis function for pions and kaons, and the double-exponential function for protons, enabling extraction of total particle yield to the full  $p_T$  region.

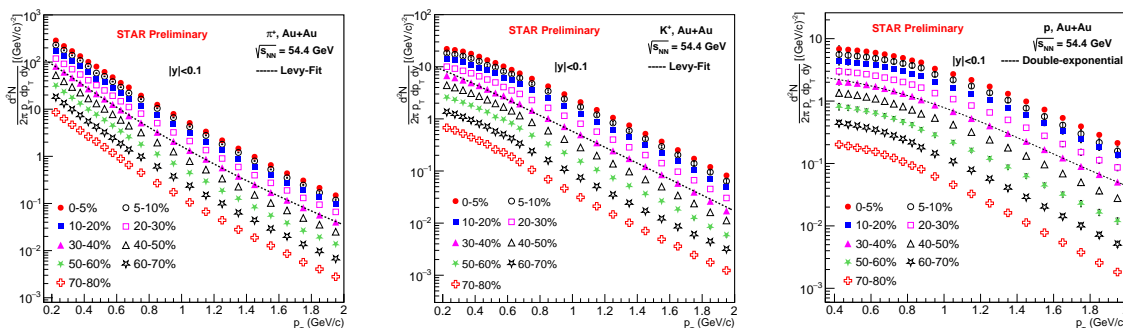


Figure 1: Transverse momentum spectra of  $\pi^+$ ,  $K^+$  and  $p$  measured in Au+Au collisions at  $\sqrt{s_{NN}} = 54.4$  GeV at mid-rapidity in STAR.

Figure 2 shows the normalized yield for different particles, demonstrating their dependencies on energy and centrality.  $\pi^+$ ,  $\pi^-$ ,  $K^+$  and  $K^-$  exhibit clear dependencies on both energy and centrality. The proton yield is maximum at 7.7 GeV and then decreases until 39 GeV, after which it slightly increases up to 200 GeV. The significant proton yield at 7.7 GeV can be attributed to the baryon stopping at lower energies, whereas as the energy increases, pair production becomes dominant. Conversely,  $\bar{p}$  displays a clear energy dependence but a weak centrality dependence. In Figure 3, the energy dependence of antiparticle-to-particle ratios is compared to global data at

44 various colliding energies [1–4]. At lower energies, the  $\pi^-/\pi^+$  ratio exceeds unity due  
 45 to isospin effects and significant contributions from resonance decays. As the energy  
 46 increases, the  $K^-/K^+$  ratio also rises, indicating a growing contribution from pair  
 47 production in kaon production. In contrast, associated production dominates at lower  
 48 energies. The energy-dependent  $\bar{p}/p$  ratio increases with rising energy, indicating  
 substantial contributions from baryon stopping at low energies.

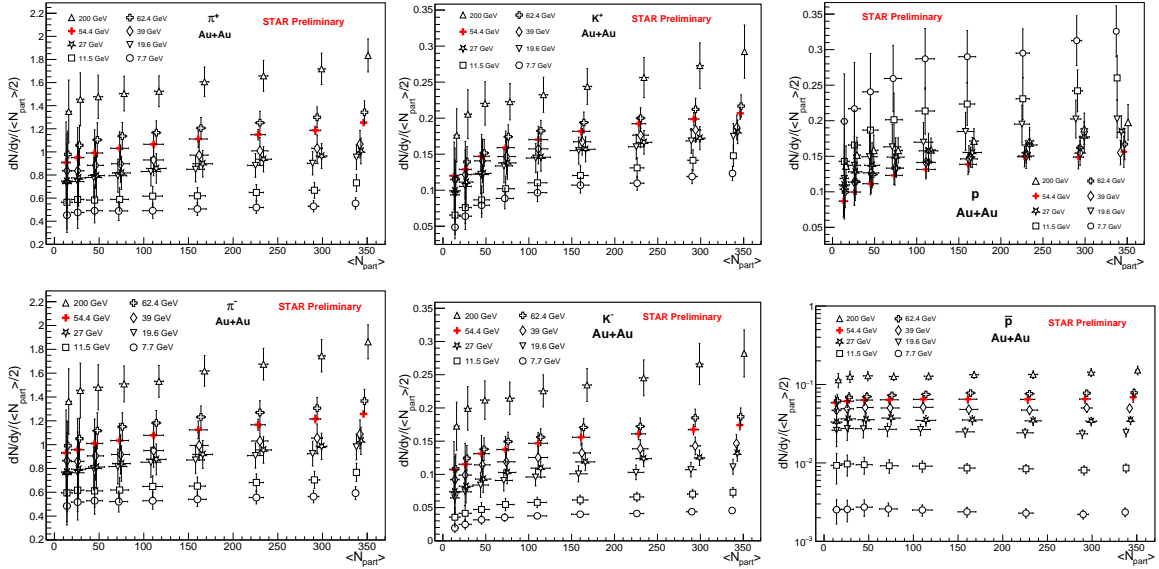


Figure 2: The normalized integrated particle yield of  $\pi^+$ ,  $\pi^-$ ,  $K^+$ ,  $K^-$ ,  $p$  and  $\bar{p}$  as a function of  $\langle N_{part} \rangle$  in Au+Au collisions at  $\sqrt{s_{NN}} = 54.4$  GeV at mid-rapidity in STAR. Results are compared to STAR published data [1, 2].

49

50 The kinetic freeze-out parameters were obtained using the hydrodynamics based  
 51 Blast-wave model [2]. The transverse momentum spectra of  $\pi^\pm$ ,  $K^\pm$ ,  $p$  and  $\bar{p}$  were  
 52 fitted simultaneously to extract the kinetic freeze-out temperature ( $T_{kin}$ ) and average  
 53 transverse radial flow velocity ( $\langle \beta \rangle$ ). Figure 4 illustrates the comparison of these re-  
 54 sults with other energy data, revealing an inverse relationship between the parameters  
 55 suggesting longer lived fireball in central collisions.

56 The Bjorken energy density provides insights into particle interactions in high-  
 57 energy collision experiments. It is defined as the energy per unit transverse area in  
 58 the transverse plane of a collision. Mathematically, it is given by the equation:

$$\epsilon_{BJ} = \frac{dE_T}{dy} \times \frac{1}{S_\perp \tau} \quad (1)$$

59 Here,  $S_{\perp}$  represents the transverse overlap area of the colliding nuclei,  $\tau$  is the forma-  
 60 tion time, and  $\frac{dE_{\perp}}{dy}$  is calculated using the integrated particle yield and mean trans-  
 61 verse momentum [2, 5, 6]. Figure 5 shows the rise in Bjorken energy density times  $\tau$   
 62 with centrality at various colliding energies (left) and an increase with collision energy  
 in the most central collisions (right).

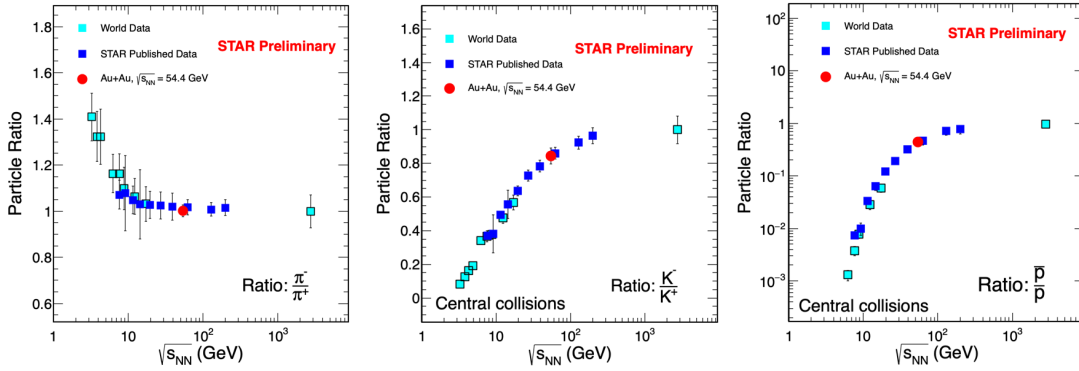


Figure 3: The anti-particle to particle yield ratio of  $\pi^-/\pi^+$ ,  $K^-/K^+$ , and  $\bar{p}/p$  as a function of energy for most central Au+Au collisions at  $\sqrt{s_{NN}} = 54.4$  GeV at mid-rapidity in STAR. Results are compared to STAR published data [1, 2] and world data. The data points corresponding to energies other than BES energies are taken from Refs. [3, 4].

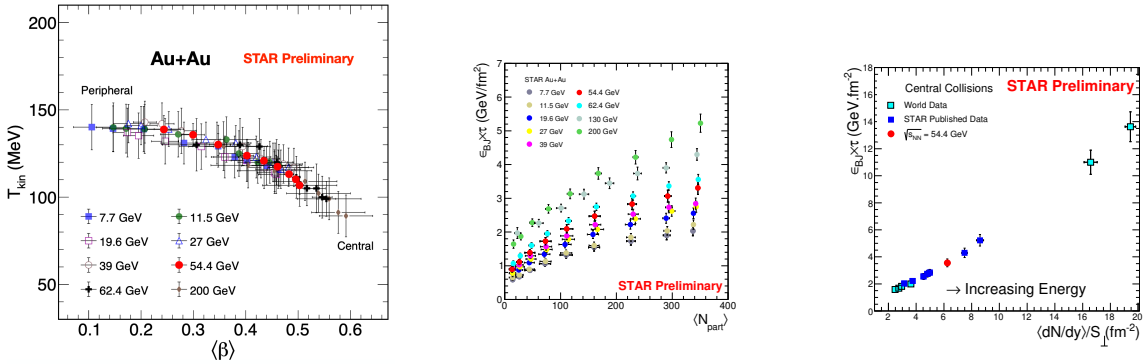


Figure 4: The variation of  $T_{kin}$  with  $\langle\beta\rangle$  in Au+Au collisions at  $\sqrt{s_{NN}} = 54.4$  GeV at mid-rapidity in STAR. Results are compared to STAR published data [1, 2].

Figure 5: Bjorken energy density times the formation time as a function of  $\langle N_{part} \rangle$  (left) and  $\langle dNdy \rangle/S_{\perp}$  (right) for Au+Au collisions at  $\sqrt{s_{NN}} = 54.4$  GeV at mid-rapidity in STAR. Results are compared to the STAR published results [1, 2] and world data [3–5].

### 3 Summary

We present measurements of identified particles ( $\pi^\pm$ ,  $K^\pm$ ,  $p$ , and  $\bar{p}$ ) at mid-rapidity ( $|y| < 0.1$ ) in Au+Au collisions at  $\sqrt{s_{NN}} = 54.4$  GeV using the STAR detector. The normalized yields of pions and kaons exhibit clear energy and centrality dependence. The proton yield peaks at 7.7 GeV, declines until 39 GeV, then experiences a slight increase up to 200 GeV. The proton yield at low energies is mainly attributed to baryon stopping and increasing energy favours the dominance of the pair production mechanism. The ratio of anti-particles to particles yields in Au+Au collisions at  $\sqrt{s_{NN}} = 54.4$  GeV follow the trend observed in worldwide data. The kinetic freeze-out parameter  $T_{kin}$ , increases from central to peripheral collisions, while  $\langle\beta\rangle$  decreases. At  $\sqrt{s_{NN}} = 54.4$  GeV, there is a two-dimensional anti-correlation between  $T_{kin}$  and  $\langle\beta\rangle$ , which follows the trend observed for other BES energies at STAR. The Bjorken energy density depicting the energy density at initial stages of collision, increases with both colliding energy and centrality.

### References

1. Adamczyk L, Adkins JK, Agakishiev G, et al. Bulk properties of the medium produced in relativistic heavy-ion collisions from the beam energy scan program. Phys. Rev. C 2017;96:044904.
2. Abelev BI et al. Systematic Measurements of Identified Particle Spectra in  $pp$ ,  $d+$  Au and Au+Au Collisions from STAR. Phys. Rev. C 2009;79:034909.
3. Abelev B, Adam J, Adamová D, et al. Centrality dependence of  $\pi$ ,  $K$ , and  $p$  production in Pb-Pb collisions at  $\sqrt{s_{NN}} = 2.76$  TeV. Phys. Rev. C 2013;88:044910.
4. Abelev BI, Aggarwal MM, Ahammed Z, et al. Identified particle production, azimuthal anisotropy, and interferometry measurements in Au + Au collisions at  $\sqrt{s_{NN}} = 9.2$  GeV. Phys. Rev. C 2010;81:024911.
5. Petrovici M, Lindner A, Pop A, Târzilă M, and Berceanu I. Geometrical scaling for energies available at the BNL Relativistic Heavy Ion Collider to those at the CERN Large Hadron Collider. Phys. Rev. C 2018;98:024904.
6. Bjorken JD. Highly relativistic nucleus-nucleus collisions: The central rapidity region. Phys. Rev. D 1983;27:140–51.